

HELIOTRON/TORSATRON CONFIGURATIONS WITH MINIMAL FIELD RIPPLES

V. Kotenko, E. Volkov, K. Yamazaki*

Institute of Plasma Physics, NSC KIPT, 61108 Kharkov, Ukraine;

**National Institute for Fusion Science, Oroshi-cho 322-6, Toki, Gifu-ken, 509-5292, Japan*

Numerical studies were undertaken to elucidate the magnetic field ripple behavior as a function of the uniform transverse magnetic field strength in the $l=2,3$ polarity helical magnetic system models, that are similar to some actual heliotron/torsatron without additional longitudinal magnetic field coils, such as LHD and U-3M. The existence of vacuum magnetic surface configurations with a minimal field ripple is demonstrated.

PACS: 52.55.Hc

INTRODUCTION

The field ripple γ ($\gamma=B_{\max}/B_{\min}$, B_{\max} , B_{\min} are the maximum and minimum magnetic field strength, respectively) on the magnetic surfaces in closed magnetic plasma traps characterizes the degree of magnetic field nonuniformity. According to the neoclassical transport theory [1], the plasma particle diffusion is supposed to be enhanced on these nonuniformities at low particle collision frequencies that are typical of the fusion reactor conditions. A few methods of decreasing the γ value have been suggested for both the tokamak magnetic systems [2-4] and the stellarator-type magnetic systems [5,6]. From the standpoint of finding magnetic configurations with a minimal γ versus the uniform transverse magnetic field, numerical calculations were carried out here to investigate helical magnetic system models with $l=2,3$ polarity, that are similar to the magnetic systems of some conventional (i.e., without additional longitudinal field coils) heliotrons/torsatrons now in operation, such as LHD [7] and U-3M [5].

GENERAL FEATURES OF CALCULATION MODELS

A poloidal cross-section $\varphi = \text{const}$. (φ is a toroidal angle) for the torus of the calculation model is schematically presented in Fig.1, where R_0 is the major radius of the torus, a is the minor radius. The electrical currents in filament-like helical conductors (not shown in Fig.1) located on the torus surface generate a longitudinal magnetic-field component b_0 on the circular axis of the system. To form closed magnetic surfaces inside the torus, it is necessary to apply a transverse magnetic field B_z , which was assumed to be uniform throughout the calculations, z being the principal (straight) torus axis. Fig.1 also shows the magnetic axis geometry. In the cases under consideration, the undistorted magnetic axis has a form of a helical line, which closes on itself after one go-round over the length of the torus and lies on the surface of an imaginary torus, the major radius of which is denoted by R_{max} (magnetic-axis major radius), and the minor radius – by r_{ax} (magnetic-axis minor radius), $R_{\text{ax}}(\varphi)$ is the radial position of magnetic axis trace in the φ poloidal cross-section. In calculations, the magnetic field line was considered closed on itself if its trace position after one go-round over the length of the torus coincided with the starting point of its calculation to an accuracy no worse than $1.0 \cdot 10^{-4}$ (here and all over the text the lengths are in R_0 units).

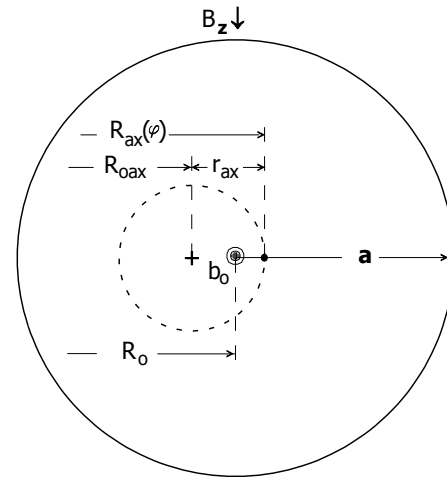


Fig.1. Torus cross-section and the magnetic axis geometry

The magnetic axis radii were defined by

$$r_{\text{ax}} = |R_{\text{ax}}(\varphi_1) - R_{\text{ax}}(\varphi_2)| / 2, R_{\text{max}} = (R_{\text{ax}}(\varphi_1) + R_{\text{ax}}(\varphi_2)) / 2, \quad (1)$$

where φ_1 , φ_2 are the toroidal angles of the poloidal cross-sections, which are spaced apart by the $1/2$ magnetic field period, and where the magnetic axis traces occur in the central plane of the torus. If $\varphi_1=0$, then $\varphi_2=180^\circ/ml$, m is the number of helical conductor pitches over the length of the torus. The magnetic field ripple values were calculated for both the magnetic axis, γ_{ax} , and the last closed magnetic surface (LCMS), γ_c . The scatter of γ_{ax} values did not exceed $1.0 \cdot 10^{-4}$. The scatter of γ_c values was about $\sim 1.2 \cdot 10^{-2}$, as the starting point of magnetic field line calculation for the LCMS identification was set to an accuracy of no better than $1.0 \cdot 10^{-3}$. The LCMS was considered existent if it showed no breakage over the length of the magnetic field line corresponding to no less than 100 go-rounds over the length of the torus. The calculation results depend on the winding law of helical conductors. To carry out the calculations, the winding law was written in a convenient explicit form:

$$\theta = \theta(m, \varphi, \alpha) = \theta_1 - k_0(\theta_2 - 2\alpha \text{arctg}(\text{tg}(\theta_1/2))), \quad (2)$$

where $0 \leq \varphi \leq 2\pi$, θ - poloidal angle, $\alpha = a/R_0$, $\theta_1 = m\varphi$ - cylindrical law of winding, $\theta_2 = 2\alpha \text{arctg}(\text{tg}(\theta_1/2))$ - equi-inclined law of winding, k_0 - numerical coefficient. For the principal values $0 \leq \varphi \leq \pi/m$ the winding law permits a simple geometric interpretation: $\theta = \theta_1 - k_0(\theta_2 - \theta_1)$. In this paper the special case $k_0=-1$, i.e., $\theta = \theta_2$, is discussed.

THE $L=2$ SYSTEM

The calculation model of the $l=2$ helical magnetic system had the following parameters: $\alpha=a/R_0=0.25$, the number of helical pitches $m=5$, the equi-inclined winding law $\theta=2\arctg(1.29099\text{tg}(2.5\varphi))$.

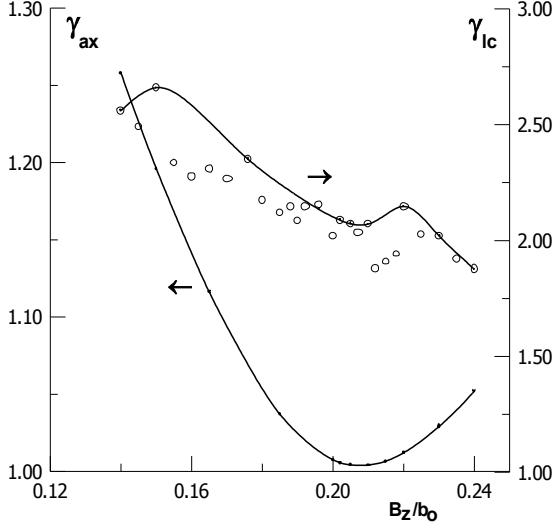


Fig. 2. Field ripples on the magnetic axis (lower solid curve), γ_{ax} , and on the LCMS, γ_c (empty circles) versus the uniform transverse magnetic field B_z in the $l=2$ system

Fig.2 presents the calculated magnetic field ripple versus the transverse magnetic field B_z (in b_0 units throughout) for the magnetic axis γ_{ax} (lower solid curve) and for the LCMS γ_c (empty circles). It is seen from the figure that the γ_{ax} curve is monotone and has a minimum in the vicinity of $B_z=(B_z)_b \approx 0.202$. The γ_c values show a wide scatter exceeding 5 to 15 times the calculation accuracy. In Fig.2 a boundary curve of the highest γ_c values is drawn. Similarly to the γ_{ax} curve, it has its minimum in the vicinity of $(B_z)_b$ but, in contrast to the γ_{ax} curve, shows a systematic falloff near the boundaries of the range of uniform transverse magnetic field variations, that most likely continues beyond the range boundaries. In the $l=2$ helical system the magnetic surface shape is stable. Therefore, the fall off of γ_c values as well as their scatter are due, first of all, to the associated changes in the LCMS average radius, as the uniform transverse magnetic field strength (or magnetic axis position, see below Fig.3) changes.

Fig.3 presents the geometrical characteristics of magnetic axes versus the transverse magnetic field B_z . From the comparison between Fig.2 and Fig.3 it follows that γ_{ax} , γ_c are minimal if the magnetic-axis minor radius of the magnetic surface configuration is equal to zero, $r_{ax}=0$ (magnetic axis is plane in principle), and the magnetic-axis major radius $(R_{oax})_b \approx 0.9594$. The existence of the plane magnetic axis follows from the fact that the difference $R_{ax}(0^\circ)-R_{ax}(18^\circ)$ in Eq.1 reverses its sign in the vicinity of the magnetic-axis major radius $(R_{oax})_b \approx 0.9594$. Obviously, the region of closed magnetic surface existence is displaced inward the torus if $(R_{oax})_b < 1$. The region of closed magnetic surface existence will be well centered, $(R_{oax})_b = 1$ for $(B_z)_b = 0.34$, if $k_0 = 0.45$ in Eq.(2):

$$\theta = 5\varphi - 0.9(\arctg(1.29099\text{tg}(2.5\varphi)) - \arctg(\text{tg}(2.5\varphi))).$$

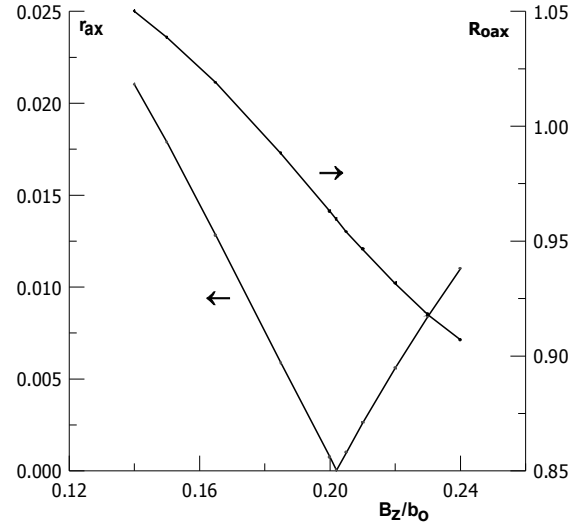


Fig. 3. Magnetic-axis minor radius r_{ax} , magnetic axis major radius R_{oax} versus the uniform transverse magnetic field B_z in the $l=2$ system

Magnetic surface parameters versus magnetic- surface average radius r for the $r_{ax}=0$ regime in the $l=2$ system show the following characteristic features: a great magnetic hill value $U \approx 0.318$, variations in the rotational transform angle i within $i \approx 0.43 \div 1.33$ (in 2π units, positive shear), and in the field ripple $\gamma \approx 1.06 \div 2.07$.

THE $L=3$ SYSTEM

The calculation model of the $l=3$ helical magnetic system had the following parameters: $\alpha = a/R_0 = 0.27$, the number of helical pitches over the length of the torus $m=3$, the equi-inclined winding law $\theta = 2\arctg(1.318987\text{tg}(1.5\varphi))$.

It is known that in toroidal $l=3$ helical magnetic systems, as the transverse magnetic field varies, a conventional magnetic surface configuration with a single undistorted (primary) magnetic axis can go over into the magnetic surface configuration with the inner island structure [8-12]. The island structure contains two magnetic axes (secondary) and an 8-shaped inner separatrix with a bifurcation line (line of hyperbolic-type singular points of the magnetic surface function). Calculations have shown that similar to the primary magnetic axis (line of elliptic-type singular points of the magnetic surface function), the bifurcation line, takes the form of the helical line which closes on itself after one go-round over the length of the torus and lies on the surface of an imaginary torus, the major radius of which is denoted as R_{olb} (bifurcation-line major radius), and the minor radius as r_{lb} (bifurcation-line minor radius); $R_{lb}(\varphi)$ is the radial position of bifurcation-line trace in the φ poloidal cross-section. The island structure is surrounded on the outside by external magnetic surfaces, which are topologically equivalent to the magnetic surfaces in the configuration with one magnetic axis. Presumably, the bifurcation line plays the role of the magnetic axis with respect to the external magnetic surfaces.

Fig.4 shows the calculated magnetic-axis minor radius r_{ax} , magnetic-axis major radius R_{oax} (solid curves), bifurcation-line minor radius r_{lb} , bifurcation-line major radius R_{olb} (dashed curves) versus the transverse magnetic field B_z in the $l=3$ system. It is seen, that at the boundaries

of the range of uniform magnetic field variations there exists the configuration with one magnetic axis. Fig 4 also shows the marked segments $(B_z)_{\text{left}}=0.289\pm 1\cdot 10^{-3}$, $(B_z)_{\text{right}}=0.367\pm 1\cdot 10^{-3}$ of the horizontal axis, within which one can observe the evidence of appearance (disappearance) of the island structure, relying on the change in the paraxial magnetic surface shape [13].

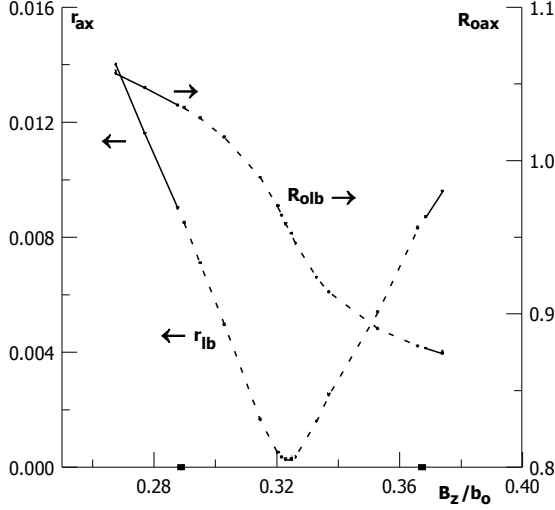


Fig. 4. Magnetic-axis minor radius r_{ax} , magnetic axis major radius R_{oax} (solid curves), bifurcation-line minor radius r_{lb} , bifurcation-line major radius R_{olb} (dashed curves) versus the uniform transverse magnetic field B_z in the $l=3$ system

The appearance (disappearance) of the island structure is evidently connected with the transitions $r_{ax}\leftrightarrow r_{lb}$, $R_{oax}\leftrightarrow R_{olb}$. Examination of Fig.4 indicates that these transitions are monotone within the accuracy of calculations. So, the central part of the range of B_z values forms the island structure configuration. For $B_z=(B_z)_b=0.325$ the island structure is maximum developed, the bifurcation-line minor radius is minimal, $r_{lb}=0.00025$ (not equal to 0 in principle, because the difference $R_{lb}(0^\circ)-R_{lb}(20^\circ)$ in Eq.(1) does not reverse its sign), the bifurcation-line major radius $R_{olb}=0.9582<1$, i.e. the magnetic surface existence region is displaced inward the torus.

Fig.5 presents the calculated magnetic field ripple versus the transverse magnetic field B_z for the magnetic axis γ_{ax} (lower solid curve), for the bifurcation line γ_b (dashed curve) and for the LCMS, γ_c (empty circles). It is seen that within the calculation accuracy, a smooth (forward and reverse) conjugation of the γ_{ax} and γ_b functions occurs within the marked segments of the B_z range. Close to $B_z=(B_z)_b$ the γ_b curve has its minimum. In contrast to the $l=2$ system, the field ripple values γ_c on the LCMS in the $l=3$ system exhibit a scatter not exceeding the calculation accuracy. This points to a monotone change in the LCMS size and shape in the $l=3$ system when the uniform magnetic field (the magnetic axis-bifurcation line position) varies. In Fig.5, the boundary of the highest γ_c values is drawn (upper solid curve). This curve, similarly to the γ_{ax} curve, has a minimum at about $(B_z)_b$ value, but in contrast to the γ_{ax} curve, it exhibits a tendency to a systematic falloff near the boundaries of the range of uniform transverse magnetic field changes, this tendency obviously becoming stronger beyond the range boundaries.

The parameters of magnetic surfaces, both inner ($r<0.05R_0$) and outer ($r>0.05R_0$) with respect to the inner separatrix, were calculated as functions of the magnetic surface average radius r in the minimum r_b regime. Inside the domain of the inner separatrix the magnetic well value is $U=0\div-0.001$, the rotational transform angle i is varying within $i\approx 0.5\div 0.3$ (in 2π units, negative shear), and the field ripple value is $\gamma\approx 1.07\div 1.15$. Outside the domain of the inner separatrix we have $U\approx 0.003\div 0.024$ (magnetic hill), $i\approx 0.125\div 0.44$ (positive shear), and $\gamma\approx 1.16\div 1.275$. Limited by the inner separatrix, the volume of the island structure takes 0.4 of the LCMS volume.

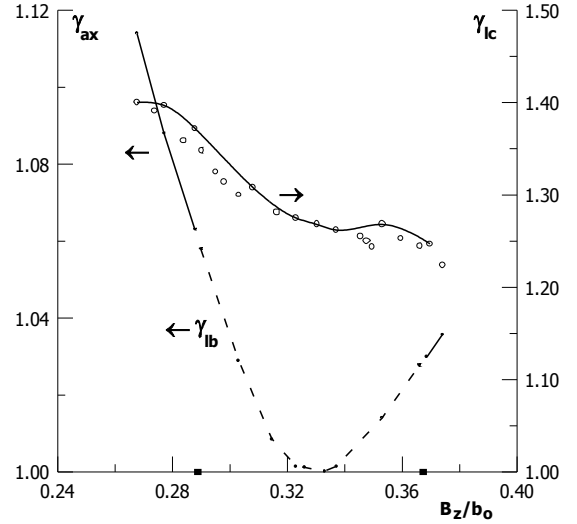


Fig. 5. Field ripples on the magnetic axis, γ_{ax} , (solid curves), on the bifurcation line, γ_b , (dashed curve) and on the LCMS, γ_c , (empty circles) versus the uniform transverse magnetic field B_z in the $l=3$ system

MAGNETIC AXIS POSITION MEASUREMENT

The localization of the magnetic axis in any poloidal cross-section may be useful for a prompt identification of a magnetic surface configuration during the running experiment. A simple scheme of measurements [14] can be of the form presented in Fig.6.

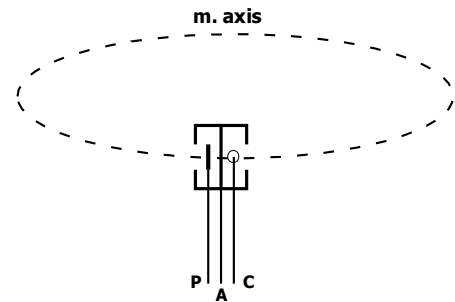


Fig.6. The scheme of magnetic axis position measurements

The basis for it is a miniature electron gun-probe (one or several). It contains a hot cathode C and a probe P on the back side of the anode box A . This probe can be made as a hot cathode and can perform its function, too, if necessary.

Owing to the possibility of decreasing essentially the electron injection potential V during probe detection of

electrons after their go-round (full or partial) along the system, one can minimize the electron trajectory distortions $\delta r \sim V^{0.5}/i$ [15,16] in order to provide high accuracy of determining the magnetic axis trace position in the chosen cross-section. Trace position of other singular, closed-on themselves field lines can also be determined with high accuracy. These may be, for example, magnetic axes and ribs of various resonance structures, as well as X-point of divertor configurations.

CONCLUSION

The numerical calculations have demonstrated the existence of the regime specified by a certain uniform transverse magnetic field value, $B_z=(B_z)_b$ in the $l=2,3$ helical systems. The field ripple on the LCMS and in the central part of the region of magnetic surface existence (magnetic axis in the $l=2$ system, bifurcation line in the $l=3$ system) is close to the minimum value in this regime. The indications of this regime are the zero minor radius of the magnetic axis ($l=2$ system), the developed inner island structure ($l=3$ system) and the minimum minor radius of the inner-separatrix bifurcation line, the displacement of region of magnetic surface existence inward the torus (in particular, for the equi-inclined law of helical conductor winding). For $B_z=(B_z)_b$, the behavior of the magnetic-surface parameters versus the magnetic-surface average radius does not differ from the standard.

Taking into account that in the straight, with undistorted helical symmetry, $l=2,3$ helical magnetic systems the magnetic axis is coincident with the geometrical axis ($r_{ax} \equiv 0$) and the field ripple value includes only the helical component (toroidal component is absent), one can assume that for fixed toroidicity the regime considered is the regime with minimum distortions of the helical-symmetry.

The calculations have also shown that the magnetic axis geometry depends on the winding law of filament-like helical conductors. Consideration must be given to the winding law of each turn in the multiturn real-size helical coil, where several parameters can vary simultaneously and insignificantly in the transition from turn to turn (e.g., k_θ and α in Eq.(2)). So, for comparison between the calculated and real parameters of the magnetic surface configuration, accurate measurements of the plane magnetic axis position become of particular importance.

ГЕЛІОТРОН-ТОРСАТРОННІ КОНФІГУРАЦІЇ З МІНІМАЛЬНИМ ПРОБКОВИМ ВІДНОШЕННЯМ

В.Г. Котенко, Є.Д. Волков, К. Ямазакі

Проведені чисельні розрахунки залежності значень пробкового відношення магнітного поля від величини однорідного поперечного магнітного поля в моделях гвинтових магнітних систем з заходністю $l=2,3$, що подібні до деяких актуальних геліотрон-торсатронних гвинтових магнітних систем, таких як LHD та У-3М. Показана можливість існування конфігурацій магнітних поверхонь з мінімальним значенням пробкового відношення.

ГЕЛИОТРОН-ТОРСАТРОННЫЕ КОНФИГУРАЦИИ С МИНИМАЛЬНЫМ ПРОБОЧНЫМ ОТНОШЕНИЕМ

В.Г. Котенко, Е.Д. Волков, К. Ямазакі

Численным методом в зависимости от величины однородного поперечного магнитного поля изучено поведение величины пробочного отношения магнитного поля в моделях винтовых магнитных систем с заходностью $l=2,3$, подобных некоторым актуальным гелиотрон-торсатронным винтовым магнитным системам без катушек продольного магнитного поля, таким как LHD и У-3М. Показана возможность существования конфигураций магнитных поверхностей с минимальным пробочным отношением.

REFERENCES

1. A.A. Galeev, R.Z.Sagdeev// *Voprosy Teorii Plasmy (Reviews of Plasma Physics)*, M: Energoatomizdat, 1973, Vol.7, pp.205-273 (in Russian).
2. N.I. Dojnikov, A.P. Lototsky, V.A. Chuanov// *Voprosy atomnoj nauki i tekhniki, Ser: Termoyad. Sint*, (4), 1987, pp. 22-26 (in Russian).
3. T. Nakayama, M. Abe, T. Tadokoray, M. Otsuka// *J.Nucl.Mat.* (491) 1999,p.271-272.
- 4.H.Kavashima, M.Sato, K.Tsazuki, et all// *Nucl. Fus.*(41), 2001, N 3, p.251-263.
- 5.O.S.Pavlichenko. A Collection of Papers Presented at the IAEA Technical Committee//*Meeting on Stellarators and Other Helical Confinement Systems at Garching, Germany 10-14 May 1993*, IAEA,Vienna, Austria, 1993, p.60.
6. V.G.Kotenko, S.S. Romanov, N.T. Besedin// *Ukr.Fiz.Zhurn.*(46), 2001, N11, p.1127-1132 (in Ukrainian).
7. O.Motojima. A Collection of Papers Presented at the IAEA Technical Committee// *Meeting on Stellarators and Other Helical Confinement Systems at Garching, Germany 10-14 May 1993*, IAEA,Vienna, Austria, 1993, p.41.
8. V.F.Aleksin// *Fizika Plazmy i problemy UTS(Plasma Physics and Problems of Controlled Thermonuclear Fusion)*,Ukr.SSR Publ., Kiev, N3,1963,p.216 (in Russian).
9. L.M. Kovrizhnykh//, *Zh.Tech. Fiz.*(33),1963,p.377(in Russian).
10. A. Gibson// *Phis. Fluids.* (10),1967,p.1553.
11. C. Gourdon, D. Marty, E.K. Maschke, J.P. Dumont// *Plasma Physics and Controlled Fusion Reserch (Proc. 3rd Int.Conf., Novosibirsk,1968)*,Vol.1,IAEA, Vienna,1969,p.847.
12. A.V. Georgievskij, V.E. Zisser, M.N. Skoblic, V.G.Peletninskaja, D.P. Pogozev, V.P. Minaev// *Voprosy atomnoj nauki i tekhniki.Ser:Fizika plazmy i problemy UTS .KFTI 73-20*, Kharkov (1) 1973,p.14 (in Russian).
13. V.N. Kaluzhnyj, V.V. Nemo// *Nucl. Fus.* (21). 1981,p.1519.
14. Patent USSR №1238009 at 12.06.1984/V. G. Kotenko (in Russian).
15. G.I. Budker// *Fiz. Plazmy i Probl. Upr. Term. Sint.*, AN USSR, Vol.1, 66,1958 (in Russian).
16. A.S. Bishop// *Phys. Fluids.*(9), 1966,p.1380.